1972

Strength of eccentrically loaded walls, February 1972 (73-51)

W. F. Chen

T. Atsuta

OFFICE
OF
RESEARCH

LEHIGH UNIVERSITY

STRENGTH OF ECCENTRICALLY LOADED WALLS

by

W. F. Chen

T. Atsuta

February 1972

Fritz Engineering Laboratory Report No. 331.20

STRENGTH OF ECCENTRICALLY LOADED WALLS

by

W. F. Chen

T. Atsuta

Fritz Engineering Laboratory
Department of Civil Engineering
Lehigh University
Bethlehem, Pennsylvania

February 1972

Fritz Engineering Laboratory Report No. 331.20

STRENGTH OF ECCENTRICALLY LOADED WALLS

by

W. F. Chen[1] and T. Atsuta[2]

Key Words: Buckling, Compression members, Concrete, Masonry, Metals, Cracking, Crushing, Eccentricity, Stability, Curvature, Beam-columns, Structural engineering

ABSTRACT: The strength of an eccentrically compressed wall is investigated by treating the wall as a beam-column. The solution adopted is the column-curvature-curve method and the strength is subject to the criteria of stability and strain limits. The material is assumed to be elastic-perfectly plastic. The yield stress levels in tension and compression may be different. Strain limits for cracking and crushing are considered. Thus, the analysis is applicable to materials such as steel, concrete and masonry. In selected cases, comparison is made with available results reported elsewhere and good agreement is observed.

[1]Associate Professor of Civil Engineering, Fritz Engineering Laboratory, Lehigh University, Bethlehem, Pa.
[2]Graduate Student, Department of Civil Engineering, Lehigh University, Bethlehem, Pa. Formerly Engineer, Kawasaki Heavy Industries, Ltd. Japan

TABLE OF CONTENTS

1. INTRODUCTION

Walls are generally treated as compression members in building design. The compressive forces may be applied eccentrically on the walls. Further, bending moments are often induced by rotation of the floor girders. The strength of a wall must hence be investigated using beam-column analysis. The ultimate strength is controlled by the stability limit or the strain limit. The Column-Curvature-Curve (CCC) method developed recently by Chen and Atsuta [2] is used herein to perform the beam-column analysis.

2. MATERIAL PROPERTIES

The material considered in this report is elastic-perfectly plastic as shown in Fig. 1.

E = modulus of elasticity

σ_{ty} = tensile yield stress (positive)

σ_{cy} = compressive yield stress (negative)

ϵ_{to} = cracking strain (positive)

ϵ_{co} = crushing strain (negative)

$$\epsilon_{ty} = \frac{\sigma_{ty}}{E} \qquad \epsilon_{cy} = \frac{\sigma_{cy}}{E} \tag{1}$$

The yield stresses and strain are defined using the ratio μ and the absolute value σ_y of the yield stress in compression.

$$\sigma_{ty} = \mu\, \sigma_y \qquad \sigma_{cy} = -\sigma_y \qquad \epsilon_y = \frac{\sigma_y}{E} \tag{2}$$

Thus, the analysis is applicable, in general, to materials which have different strengths in tension and in compression.

For idealized steel $\mu = 1$

For idealized masonry $\mu = 0$ (3)

For idealized concrete $0 < \mu < 1$

3. MOMENT-CURVATURE-THRUST RELATIONSHIP

The wall has the thickness t and the height h as shown in Fig. 2. The loads are the axial force P on the midthickness and the two end moments M_A and M_B.

The material properties, the geometry and the loads are considered invariant along the width. Hence, a wall with a unit width is considered in this report. Therefore, it is the same as a rectangular beam-column of depth t, width 1.0 and length h.

It is assumed that plane sections remain plane after deformation. Thus the strain distribution is linear through the wall thickness. In terms of the mean strain ϵ_m and the curvature Φ (Fig. 3), the strain ϵ at location y from center line is

$$\epsilon = \Phi y + \epsilon_m \tag{4}$$

The boundaries of compression yield y_{cy} and tension yield y_{ty} are given by

$$y_{ty} = \frac{1}{\Phi}(\epsilon_{ty} - \epsilon_m) \qquad y_{cy} = \frac{1}{\Phi}(\epsilon_{cy} - \epsilon_m) \tag{5}$$

Eq. 5 has meaning only for

$$-\frac{t}{2} \le y_{ty} \le \frac{t}{2} \qquad -\frac{t}{2} \le y_{cy} \le \frac{t}{2} \tag{6}$$

The stress is given by

$$\sigma = \begin{cases} \sigma_{cy} & (y \le y_{cy}) \\ E\ (\Phi y + \epsilon_m) & (y_{cy} \le y \le y_{ty}) \\ \sigma_{ty} & (y_{ty} \le y) \end{cases} \tag{7}$$

In order to derive simple expressions for axial force P and bending moment M, the following specially defined parentheses are convenient for use.

$$< S > = \begin{cases} S & (0 \le S) \\ 0 & (S \le 0) \end{cases} \tag{8}$$

Axial force and bending moment per unit width are

$$P = \int_{-\frac{t}{2}}^{\frac{t}{2}} \sigma dy \qquad M = \int_{-\frac{t}{2}}^{\frac{t}{2}} \sigma y dy \tag{9}$$

Using Eqs. 7, 8 and 9

$$P = \int_{-\frac{t}{2}}^{\frac{t}{2}} (E\Phi y + E\epsilon_m)\, dy - \int_{-\frac{t}{2}}^{\frac{t}{2}} <-E\Phi y - E\epsilon_m + \sigma_{cy}>\, dy - \int_{-\frac{t}{2}}^{\frac{t}{2}} <E\Phi y + E\epsilon_m - \sigma_{ty}>\, dy \tag{10a}$$

$$M = \int_{-\frac{t}{2}}^{\frac{t}{2}} (E\Phi y + E\epsilon_m)\, y dy + \int_{-\frac{t}{2}}^{\frac{t}{2}} <-E\Phi y - E\epsilon_m + \sigma_{cy}>\, y dy - \int_{-\frac{t}{2}}^{\frac{t}{2}} <E\Phi y + E\epsilon_m - \sigma_{ty}>\, y dy \tag{10b}$$

These may now be reduced to two simple equations using Eqs. 2, 5 and 8 (Fig. 3),

$$P = E\epsilon_m t + \frac{E}{2\Phi} <\frac{\Phi t}{2} - \epsilon_y - \epsilon_m>^2 - \frac{E}{2\Phi} <\frac{\Phi t}{2} - \mu\epsilon_y + \epsilon_m>^2 \tag{11a}$$

$$M = \frac{E\Phi t^3}{12} - \frac{E}{6\Phi^2} <\frac{\Phi t}{2} - \epsilon_y - \epsilon_m>^2 (\Phi t + \epsilon_y + \epsilon_m) - \frac{E}{6\Phi^2} <\frac{\Phi t}{2} - \mu\epsilon_y + \epsilon_m>^2 (\Phi t + \mu\epsilon_y - \epsilon_m) \tag{11b}$$

The equations are next simplified using non-dimensionalized quantities

$$\bar{\sigma} = \frac{\sigma}{\sigma_y} \qquad \bar{\epsilon} = \frac{\epsilon}{\epsilon_y} \tag{12}$$

$$p = -\frac{P}{P_y} \qquad m = \frac{M}{M_y} \qquad \varphi = \frac{\Phi}{\Phi_y} \tag{13}$$

where

$$P_y = \sigma_y t \qquad M_y = \sigma_y \frac{t^2}{6} \qquad \Phi_y = \epsilon_y \frac{2}{t} \tag{14}$$

Also, henceforth, a positive value for p indicates compressive force. Thus Eq. 11 becomes

$$P = -\bar{\epsilon}_m - \frac{1}{4\varphi}\left[\langle\varphi-1-\bar{\epsilon}_m\rangle^2 - \langle\varphi-\mu+\bar{\epsilon}_m\rangle^2\right] \tag{15a}$$

$$m = \varphi - \frac{1}{4\varphi^2}\left[\langle\varphi-1-\bar{\epsilon}_m\rangle^2\ (2\varphi+1+\bar{\epsilon}_m) + \langle\varphi-\mu+\bar{\epsilon}_m\rangle^2\ (2\varphi+\mu-\bar{\epsilon}_m)\right] \tag{15b}$$

Elimination of $\bar{\epsilon}_m$ from Eqs. 15(a) and 15(b) yields a relationship among the bending moment m, the curvature φ and the thrust p in the elastic as well as elastic-plastic regimes.

Since direct elimination is not possible, the m-φ-p equations are derived in four different regimes separately (Fig. 4).

(a) Elastic Regime ($\varphi \le \varphi_{et}$ and $\varphi \le \varphi_{ec}$)

$$\bar{\epsilon}_m = -p \tag{16a}$$

$$m = \varphi \tag{16b}$$

(b) Tension Yield Regime ($\varphi_{et} \le \varphi_{ec}$ and $\varphi_{et} < \varphi \le \varphi_{tc}$)

$$\bar{\epsilon}_m = \varphi + \mu - 2\sqrt{\varphi\ (\mu+p)} \tag{17a}$$

$$m = 3\ (\mu+p) - 2\sqrt{\frac{(\mu+p)^3}{\varphi}} \tag{17b}$$

(c) Compression Yield Regime ($\varphi_{ec} < \varphi_{et}$ and $\varphi_{ec} < \varphi \leq \varphi_{ct}$)

$$\bar{\epsilon}_m = -(1+\varphi) + 2\sqrt{\varphi(1-p)} \tag{18a}$$

$$m = 3(1-p) - 2\sqrt{\frac{(1-p)^3}{\varphi}} \tag{18b}$$

(d) Combined Yield Regime ($\varphi_{tc} < \varphi$ or $\varphi_{ct} < \varphi$)

$$\bar{\epsilon}_m = \frac{\varphi}{1+\mu}(1-\mu-2p) - \frac{1-\mu}{2} \tag{19a}$$

$$m = 3\frac{(1-p)(\mu+p)}{1+\mu} - \frac{(1+\mu)^3}{16\varphi^2} \tag{19b}$$

In the present analysis, only positive curvature is taken into account without violating the generality. The boundary curvatures used in Eqs. 16 to 19 are given by

$$\begin{aligned}
\varphi_{et} &= \mu + p && \text{(Elastic-tension Yield)} \\
\varphi_{ec} &= 1 - p && \text{(Elastic-compression Yield)} \\
\varphi_{tc} &= \frac{(1+\mu)^2}{4(\mu+p)} && \text{(Tension-compression Yield)} \\
\varphi_{ct} &= \frac{(1+\mu)^2}{4(1-p)} && \text{(Compression-tension Yield)}
\end{aligned} \tag{20}$$

The order in which the different distributions of stress as shown in Fig. 4(a), 4(b), 4(c) and 4(d) may occur with increasing φ is of importance in the analysis. If the section is elastic throughout under thrust p alone, its behavior under the bending moment m is initially governed by Fig. 4(a). The addition of the moment m will increase φ and for some value of m, the section will start to yield. Assuming the tension fibers begin to yield first, the behavior is now governed by Fig. 4(b), and the boundary curvature between Fig. 4(a) and Fig. 4(b) is φ_{et}. If the curvature φ can further be increased to φ_{tc},

the compression fibers also begin to yield and for any value of $\varphi > \varphi_{tc}$ the behavior of the section is governed by Fig. 4(d). By similar reasoning, the other sequence of yielding is Fig. 4(a), 4(c) and finally 4(d) and the corresponding boundary curvatures between Fig. 4(a) and 4(c) and between Fig. 4(c) and 4(d) are φ_{ec} and φ_{ct} respectively.

Comparing the two initial yield curvatures φ_{et} and φ_{ec}, it is known that

$$\begin{aligned} &\text{if } p < \frac{1-\mu}{2}, \text{ tension yielding occurs first} \\ &\text{if } p > \frac{1-\mu}{2}, \text{ compression yielding occurs first} \end{aligned} \tag{21}$$

Using this relationship, Eq. 20 can be simplified to

$$\begin{aligned} \varphi_{et},\ \varphi_{ec} &= \frac{1+\mu}{2} - \left| \frac{1-\mu}{2} - p \right| = \varphi_1 \\ \varphi_{tc},\ \varphi_{ct} &= \frac{(1+\mu)^2}{4\varphi_1} \qquad\qquad = \varphi_2 \end{aligned} \tag{22}$$

Now there are only three regimes:

(a) Elastic Regime $(\varphi \le \varphi_1)$

$$m = a\,\varphi \tag{23}$$

(b) Tension or Compression Yield Regime $(\varphi_1 < \varphi \le \varphi_2)$

$$m = b - \frac{c}{\sqrt{\varphi}} \tag{24}$$

(c) Combined Yield Regime $(\varphi_2 < \varphi)$

$$m = m_{pc} - \frac{f}{\varphi^2} \tag{25}$$

where

$$\begin{aligned} a &= 1 \qquad & b &= 3\varphi_1 \qquad & c &= 2\varphi_1^{3/2} \\ f &= \frac{(1+\mu)^3}{16} \qquad & m_{pc} &= 3\,\frac{(1-p)(\mu+p)}{1+\mu} \end{aligned} \tag{26}$$

The m-φ-p relationships derived in Ref. 1 and 2 for steel beam-columns and in Refs. 3 and 4 for plain concrete and masonry walls are special cases of Eqs. 23 to 26 with $\mu = 1.0$ and $\mu = 0$ respectively.

4. STRAIN LIMITS

As one of the strength criteria, the wall is assumed to reach its ultimate state when the strain at the extreme fiber reaches the strain limit of the material. The strain limits are

$$\begin{aligned} \varepsilon_{co} &= \text{crushing strain (negative)} \\ \varepsilon_{to} &= \text{cracking strain (positive)} \end{aligned} \tag{27}$$

Since the strain distribution is given by Eq. 4, these conditions are reached when

$$\begin{aligned} \varepsilon_{co} &= -\frac{\phi t}{2} + \varepsilon_m \\ \varepsilon_{to} &= \frac{\phi t}{2} + \varepsilon_m \end{aligned} \tag{28}$$

or non-dimensionally

$$\bar{\varepsilon}_m = \begin{cases} \bar{\varphi} + \bar{\varepsilon}_{co} \\ -\bar{\varphi} + \bar{\varepsilon}_{to} \end{cases} \tag{29}$$

Substituting this $\bar{\varepsilon}_m$ into Eqs. 16 to 19, the cracking curvature φ_{to} and crushing curvature φ_{co} are obtained as follows:

(a) Elastic Regime ($\varphi_{to} \le \varphi_1$, $\varphi_{co} \le \varphi_1$)

$$\begin{aligned} \varphi_{to} &= \bar{\varepsilon}_{to} + p \\ \varphi_{co} &= -(\bar{\varepsilon}_{co} + p) \end{aligned} \tag{30}$$

(b) Tension or Compression Yield Regime ($\varphi_1 < \varphi_{to} \le \varphi_2, \varphi_1 < \varphi_{co} \le \varphi_2$)

$$\begin{aligned} \varphi_{to} &= \frac{\bar{\varepsilon}_{to}+p}{2} + \frac{1}{2}\sqrt{(\bar{\varepsilon}_{to}+p)^2 - (\mu-\bar{\varepsilon}_{to})^2} \\ \varphi_{co} &= -\frac{(\bar{\varepsilon}_{co}+p)}{2} + \frac{1}{2}\sqrt{(\bar{\varepsilon}_{co}+p)^2 - (1+\bar{\varepsilon}_{co})^2} \end{aligned} \tag{31}$$

(c) Combined Yield Regime $(\varphi_2 < \varphi_{to}, \varphi_2 < \varphi_{co})$

$$\varphi_{to} = \frac{1}{1-p}\left(\frac{1+\mu}{2}\bar{\varepsilon}_{to} + \frac{1-\mu^2}{4}\right)$$
$$\varphi_{co} = \frac{-1}{\mu+p}\left(\frac{1+\mu}{2}\bar{\varepsilon}_{co} + \frac{1-\mu^2}{4}\right) \tag{32}$$

5. COLUMN-CURVATURE CURVES

For a beam-column AB of length L which is subjected to an axial force P, bending moments M_A and M_B at the ends, there is an equivalent column of length L* which is subjected only to the axial force

$$P^* = \sqrt{P^2 + \left(\frac{M_A - M_B}{L}\right)^2} \tag{33}$$

The beam-column AB is a part of its equivalent column A*B* as shown in Fig. 5. The proof is presented in Ref. 2.

Since the end curvatures $\bar{\Phi}_A$ and $\bar{\Phi}_B$ are known from end moments M_A and M_B, using the previously obtained moment-curvature-thrust relationship, the curvature distribution along the beam-column AB is determined if the curvature distribution of the equivalent column A*B* (the column curvature curves) is known (Fig. 6).

The column curvature curves were obtained in Ref. 2, and the procedure is briefly given here. There are five different types of equivalent columns as shown in Fig. 7. The governing equation of a beam-column is

$$\frac{d^2M}{dx^2} + k^2\bar{\Phi} = 0 \tag{34}$$

in which

$$k = \sqrt{\frac{P^*}{EI}} \tag{35}$$

$$EI = \frac{Et^3}{12} \qquad \text{(bending rigidity)} \tag{36}$$

Using the previously derived moment-curvature-thrust relationships, (Eqs. 23, 24, and 25), Eq. 34 may be reduced to a set of differential equations in Φ and P only [2].

For each type of column shown in Fig. 7, the curvature φ is not solved explicitly. Instead kx is obtained as a function of φ. In the solution, the maximum curvature at the center φ_m^* is included as an integral constant. Details of the solution for each case have been reported elsewhere [2].

(a) Elastic Column $(\varphi_m^* \leq \varphi_1)$

$$kL^* = \pi\sqrt{a} \tag{37}$$

$$kx = \frac{kL^*}{2} - f_1\left(\sqrt{a},\ \varphi,\ \varphi_m^*,\ \frac{kL^*}{2}\right) \tag{38}$$

(b) One Side Plastic Column $(\varphi_1 < \varphi_m^* \leq \varphi_2)$

$$k\rho_1 = g\left(\sqrt{a},\ c,\ \varphi_1,\ \varphi_m^*\right) \tag{39}$$

$$kL^* = 2k\rho_1 + 2f_2\left(c,\ \varphi_m^*,\ \varphi_1\right)$$

$$kx = \begin{cases} \dfrac{kL^*}{2} - f_1\left(\sqrt{a},\ \varphi,\ \varphi_1,\ k\rho_1\right) & (\varphi \leq \varphi_1) \\ f_2\left(c,\ \varphi_m^*,\ \varphi\right) & (\varphi_1 < \varphi) \end{cases} \tag{40}$$

(c) Combined Plastic Column $(\varphi_2 < \varphi_m^*)$

$$\varphi_o = \left[\sqrt{\varphi_2} + \frac{2f}{c}\left(\frac{1}{\varphi_2} - \frac{1}{\varphi_m^*}\right)\right]^2$$

$$k\rho_1 = g\left(\sqrt{a},\ c,\ \varphi_1,\ \varphi_o\right)$$

$$k\chi_p = k\rho_1 + f_2\ (c,\ \varphi_o,\ \varphi_1) \tag{41}$$

$$k\rho_2 = k\chi_p - f_2\ (c,\ \varphi_o,\ \varphi_2)$$

$$kL^* = 2k\rho_2 + 2f_3\ (f,\ \varphi_2,\ \varphi_m^*)$$

$$k\chi = \begin{cases} \dfrac{kL^*}{2} - f_1\ (\sqrt{a},\ \varphi,\ \varphi_1,\ k\rho_1) & (\varphi \le \varphi_1) \\ \dfrac{kL^*}{2} - k\chi_p + f_2\ (c,\ \varphi_o,\ \varphi) & (\varphi_1 < \varphi \le \varphi_2) \\ f_3\ (f,\ \varphi,\ \varphi_m^*) & (\varphi_2 < \varphi) \end{cases} \tag{42}$$

where the functions are given by

$$f_1\ (\sqrt{a},\ \varphi,\ \varphi_1,\ k\rho) = \sqrt{a}\ \sin^{-1}\left(\frac{\varphi}{\varphi_1}\ \sin\frac{k\rho}{\sqrt{a}}\right)$$

$$f_2\ (c,\ \varphi_o,\ \varphi) = \sqrt{\frac{c}{2}}\ \varphi_o^{-3/4}\left[\sqrt{\frac{\varphi_o}{\varphi}\left(1-\sqrt{\frac{\varphi}{\varphi_o}}\right)} + \tanh^{-1}\sqrt{1-\sqrt{\frac{\varphi}{\varphi_o}}}\right]$$

$$f_3\ (f,\ \varphi,\ \varphi_m) = \frac{2}{3}\sqrt{\frac{f}{\varphi} - \frac{f}{\varphi_m}}\left(\frac{2}{\varphi_m} + \frac{1}{\varphi}\right) \tag{43}$$

$$g\ (\sqrt{a},\ c,\ \varphi_1,\ \varphi_m) = \sqrt{a}\ \tan^{-1}\frac{\sqrt{a}\ \varphi_1}{\sqrt{2c\ (\sqrt{\varphi_m}-\sqrt{\varphi_1})}}$$

Figure 8 shows a set of such column curvature curves obtained from Eqs. 37 to 43 for a wall of $\mu = 0$ and $p = 0.2$.

6. METHOD OF SOLUTION

If the maximum column curvature φ_m^* is known, the location x_A and x_B corresponding to the end curvatures φ_A and φ_B are obtained exactly from Eqs. 38, 40 and 42. The actual value of φ_m^* must be searched by iteration until the computed length L_{AB} between x_A and x_B becomes close to the length L of the beam-column.

$$L_{AB} \approx L \tag{44}$$

The length L_{AB} is computed in four different cases as shown in Fig. 9. In each case, the maximum curvature of the beam-column φ_m and its location x_m are given by the following equations.

(a) Single Curvature $(\varphi_A \varphi_B \geq 0)$

$$\text{Type 1} \quad L_{AB} = x_B - x_A$$
$$\varphi_m = \varphi_A, \; x_m = 0 \tag{45}$$

$$\text{Type 2} \quad L_{AB} = x_B + x_A$$
$$\varphi_m = \varphi_m^*, \; x_m = x_A \tag{46}$$

(b) Double Curvature $(\varphi_A \varphi_B < 0)$

$$\text{Type 1} \quad L_{AB} = L^* - x_A - x_B$$
$$\varphi_m = \varphi_A, \; x_m = 0 \tag{47}$$

$$\text{Type 2} \quad L_{AB} = L^* + x_A - x_B$$
$$\varphi_m = \varphi_m^*, \; x_m = x_A \tag{48}$$

In the above derivation, it is assumed (without loss of generality) that

$$\left| \varphi_B \right| \leq \varphi_A \tag{49}$$

7. NUMERICAL EXAMPLES

Results of some numerical calculations are presented in Figs. 10 and 11. The ordinate is the axial force p and the

abscissa is the maximum curvature of the wall φ_m. The p-φ_m planes are divided by the two dotted lines φ_1 and φ_2 into four regimes: the elastic regime, tension yield regime, compression yield regime and the combined yield regime. The thick solid lines represent load curvature curves for various slenderness ratios of h/t. Each curve consists of a loading portion and an unloading portion. The peak points indicate the stability limit of the walls. Strain limits are plotted by thin solid lines.

The stability limits (peak points) occur just after tension yield. Unloading takes place mostly in the combined yield regime except for tall walls with no tensile strength ($\mu = 0$, $h/t > 30$).

Figure 12 shows stability limits of walls with varying tensile strength ($\mu = 0$ to 1.0). It should be noted here that a small amount of tensile strength ($\mu = 0.1$) improves the strength of walls considerably. Thus the tensile yield stress should not be neglected in analysis of plain concrete or masonry walls.

Tensile yield stress greater than half of compressive yield stress ($\mu > 0.5$) has no effect except for very short walls ($h/t < 10$).

Figures 13 and 14 show the ultimate strength of a wall due to strain limits of $\mu = 0$ and $\mu = 0.1$ respectively. The thick solid line shows the stability limit. The dotted lines and thin solid lines represent crushing failure and cracking failure, respectively.

Crushing occurs only in shorter walls but cracking occurs in most walls. A small amount of ductility improves the strength of the wall considerably. This effect is noticeable especially during cracking in masonry wall (Fig. 13). Large ductility ($\varepsilon_{to} > 0.5\ \varepsilon_y$ $|\varepsilon_{co}| > 2\varepsilon_y$)

has little effect on strength of walls.

Figure 15 shows the stability limit of a wall (μ = 0 and 0.1) against different types of loading. The parameter α is ratio of end moments ($\alpha = m_B/m_A$). Three loading cases are investigated: symmetric loading (α = 1), one moment loading (α = 0) and antisymmetric loading (α = -1).

The strength of the wall under unsymmetric loading (α =0, -1) is considerably greater than that in the symmetric case. This is because of the difference in the critical length. Also, in these cases, the plastic hinge occurs at an end and the strength becomes constant when the wall is short (Fig. 15).

8. COMPARISON WITH REPORTED RESULTS

In Ref. 4, ultimate strengths of walls are reported. The material has no tensile strength (μ = 0). The compressive strain limit is the same as the initial yield strain ($\varepsilon_{co} = -\varepsilon_y$) and the tensile strain limit is not defined ($\varepsilon_{to} = \infty$). The loading is symmetric (α = 1) but eccentricity of the axial force is variable (e = t/6 and e = t/3 are taken in the example). The yield strain is ε_y = 0.001215 in pure compression. Strength in flexure is 1.6 times the strength in pure compression (ε_y = 0.001944). Results of Ref. 4 are plotted by circles in Fig. 16.

To recompute these results using the approach here, the ultimate strength of the walls is investigated in four cases

In Fig. 16, the solid curves (a) and (b)

represent stability limits of the walls with $\varepsilon_y = 0.001215$ and $\varepsilon_y = 0.001944$, respectively. Since there are strain limits ($\varepsilon_{co} = -\varepsilon_y$), the strengths are reduced to the dotted lines (a') and (b'). Applying the factor 1.6 to the p-value of curve (b'), the crushing strength curve (c) is obtained. The ultimate strength is represented by the stability part of curve (a) and crushing part of curve (c). Figure 16 shows good agreement between the two results in both cases of eccentricity.

9. SUMMARY AND CONCLUSIONS

A method to analyze strength of walls of general materials is presented. An elastic-perfectly plastic material is considered. The yield stresses and limit strains in tension and compression may be different. In the analysis, the column-curvature-curve method is used.

The loadings are axial compression and bending moments at the ends, which may be unsymmetric. Further, the end moments are not necessarily due to eccentricity of the axial force, they may be applied independently.

The small tensile strength and ductility of plain concrete or masonry are found to have a significant effect on the strength of walls and should not be neglected in analysis. For plain concrete or masonry walls, compressive ductility greater than twice the initial yield strain ε_y and tensile ductility greater than half the initial yield strain ε_y are desirable features.

A good agreement was observed in some special cases with other reported results.

10. ACKNOWLEDGMENTS

The junior writer is grateful to Kawasaki Heavy Industries, Ltd., Japan for providing him with the opportunity to study at Lehigh University. The preparation of this report was sponsored by the National Science Foundation under grant GK-14274 to Lehigh University. All computations were made at the Computer Center through the Department of Civil Engineering, Lehigh University.

11. REFERENCES

1. Chen, W. F. and Santathadaporn, S.
"Curvature and Solution of Eccentrically Loaded Columns", Journal of the Engineering Mechanics Division, ASCE, Vol. 95, No. EM 1, February 1969, pp. 21-39.

2. Chen, W. F. and Atsuta, T.
"Column Curvature Curve Method for Analysis of Beam Columns", The Institution of Structural Engineers, London, England, June 1972. (in press)

3. Chen, W. F.
Discussion of "Stability and Load Capacity of Members with No Tensile Strength", by F. Y. Yokel, Journal of the Structural Division, ASCE, Vol. 98, No. ST5, May 1972. (in press)

4. Yokel, F. Y.
"Stability and Load Capacity of Members with No Tensile Strength", Journal of the Structural Division, ASCE, Vol. 97, No. ST7, July 1971, pp. 1913-1926.

12. NOTATIONS

a, b, c, f, m_{pc} = constants which determine m-φ-p relationship

e = eccentricity of axial thrust P

E = modulus of elasticity

f_1, f_2, f_3, g = functions which determine CCC (Eq. 43)

h = height of wall

I = moment of interia of cross section ($= \frac{t^3}{12}$)

k = $\sqrt{P^*/EI} = \sqrt{12\ \varepsilon_y\ P^*}/t$

L = length of beam-column

L^* = length of equivalent column

L_{AB} = computed distance between A and B

$M, (m)$ = bending moment ($m = M/M_y$)

$M_A, M_B, (m_A, m_B)$ = end moments ($m_A = M_A/M_y$, $m_B = M_B/M_y$)

M_y = initial yield moment ($= \sigma_y\ t^2/6$)

$P, (p)$ = axial thrust ($p = -P/P_y$)

P_y = yield thrust ($= \sigma_y\ t$)

$P^*, (p^*)$ = thrust in equivalent column ($p^* = P^*/P_y$)

t = thickness of wall

V = shear force in beam-column

x, y = coordinate along and across wall height

x_m = location of maximum curvature

y_{ty}, y_{cy} = boundary of yielding in tension and compression

$\varepsilon, (\bar{\varepsilon})$ = axial strain ($\bar{\varepsilon} = \varepsilon/\varepsilon_y$)

$\varepsilon_{ty}, \varepsilon_{cy}$ = yield strain in tension and compression

$\varepsilon_{to}, \varepsilon_{co}$ = limit strains (cracking and crushing)

ε_y = yield strain ($= \sigma_y/E$)

ε_m = mean strain

χ = M_B/M_A

μ = $-\sigma_{ty}/\sigma_{cy}$

σ, $(\bar{\sigma})$ = axial stress $(\bar{\sigma} = \sigma/\sigma_y)$

σ_{ty}, σ_{cy} = yield stress in tension and compression

σ_y = yield stress (= $|\sigma_{cy}|$)

$\varphi_{et}, \varphi_{ec}, \varphi_{tc}, \varphi_{ct}$ = boundary curvatures

φ_1, φ_2 = boundary curvatures

φ_{to}, φ_{co} = ultimate curvatures due to strain limit

φ_m, φ_m^* = maximum curvatures in wall and in equivalent column

φ_A, φ_B = end curvatures

Φ, (φ) = curvature $(\varphi = \Phi/\Phi_y)$

Φ_y = initial yield curvature (= $2\varepsilon_y/t$)

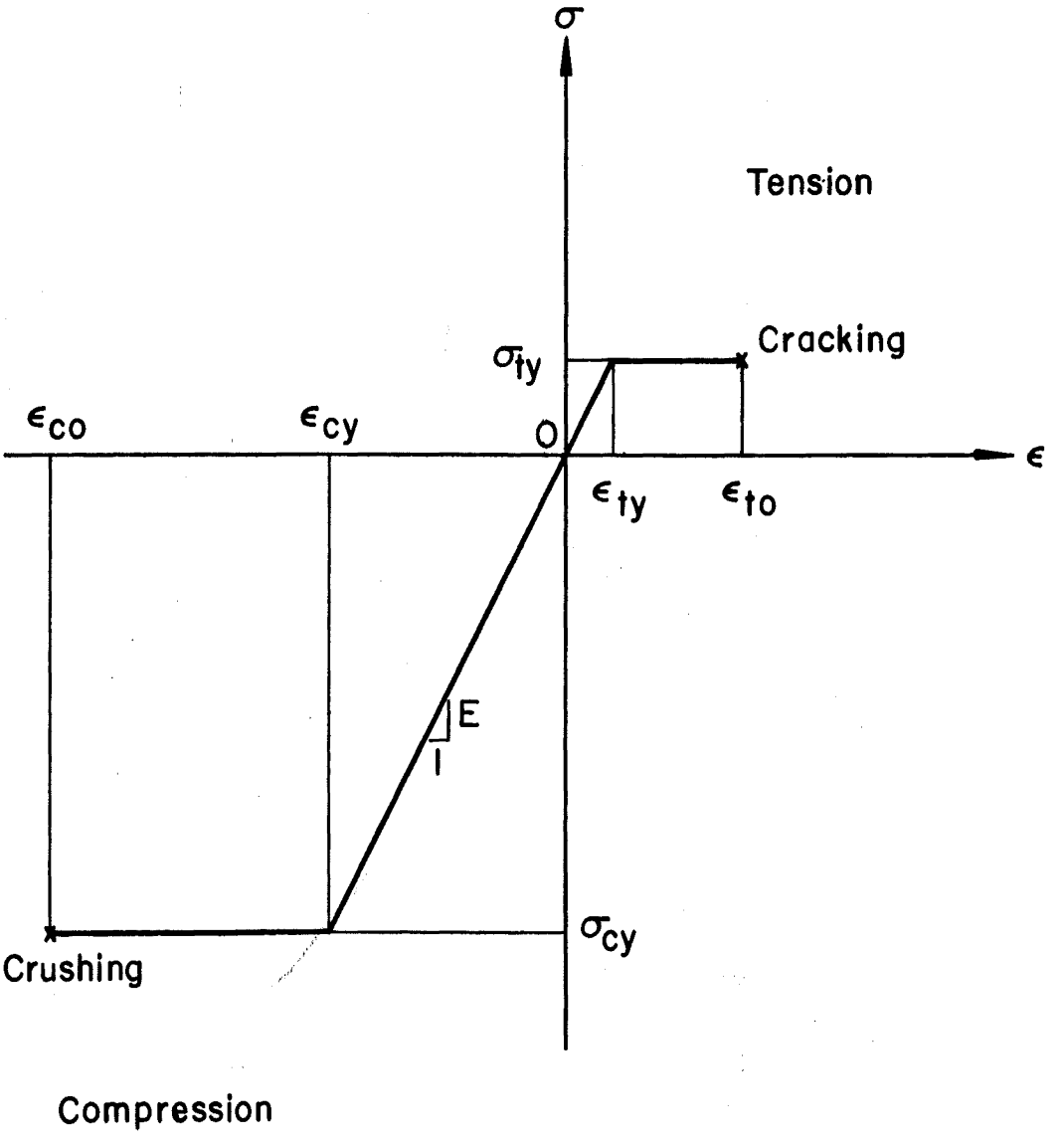

Fig. 1 Idealized Stress-Strain Relationship

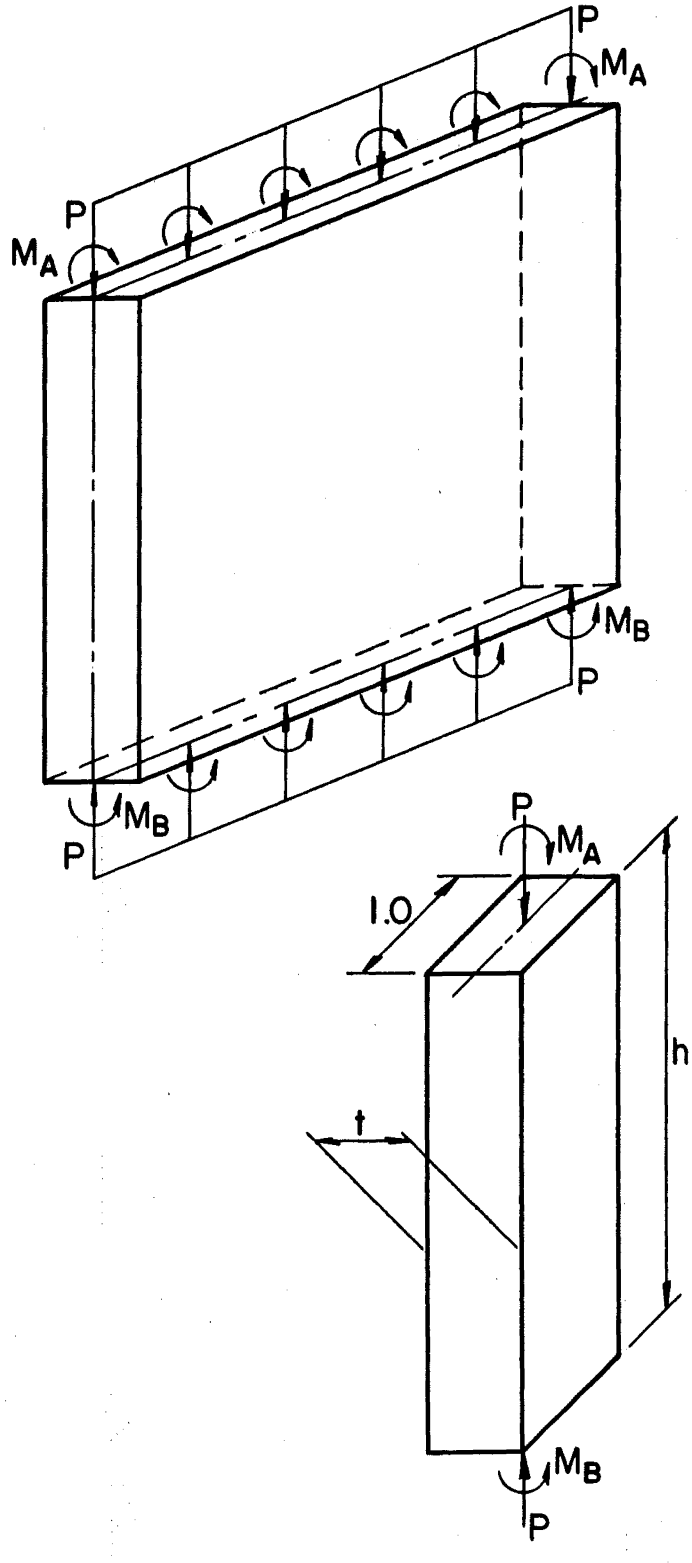

Fig. 2 Wall and Beam-Column

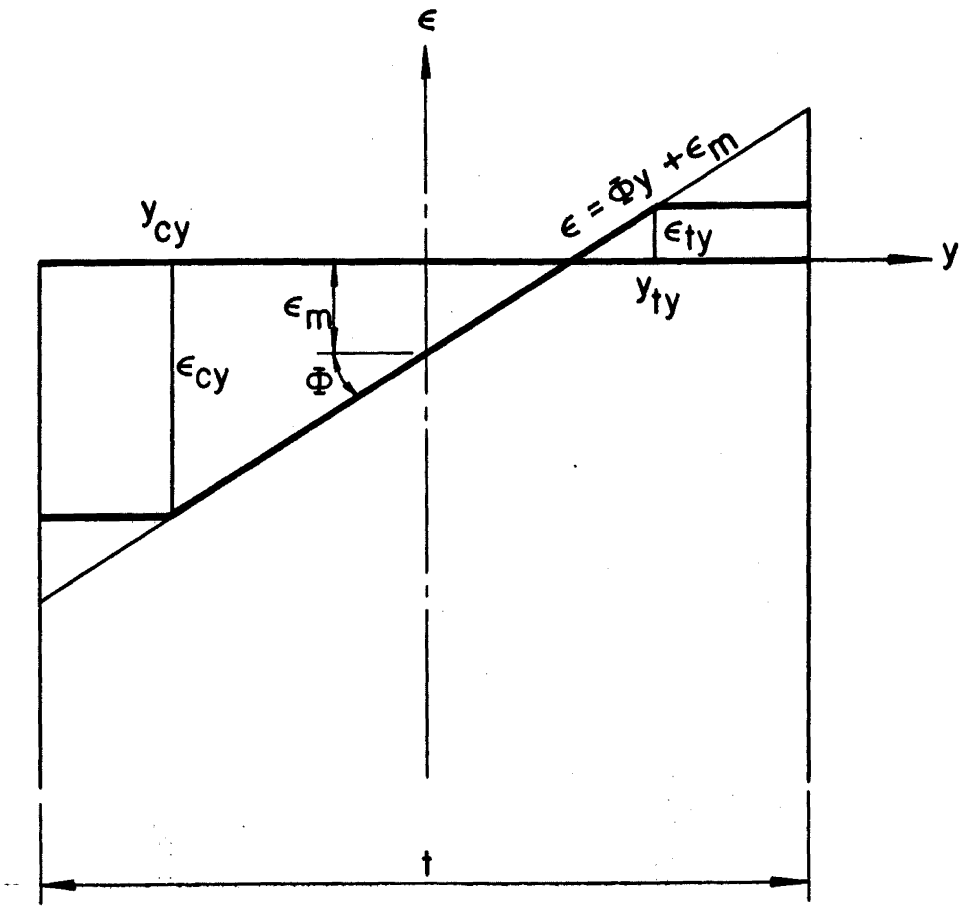

Fig. 3 Linear Distribution of Strain

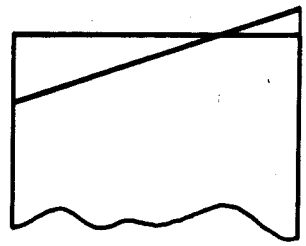

(a) Elastic Regime

$(\phi \le \phi_{et} \quad \phi \le \phi_{ec})$

$$m = \phi$$

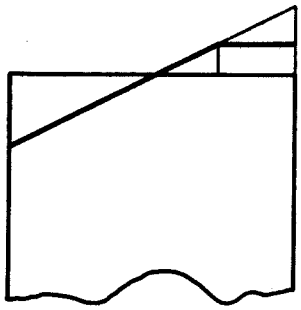

(b) Tension Yield Regime

$(\phi_{et} < \phi_{ec} \quad \phi_{et} < \phi \le \phi_{tc})$

$$m = 3(\mu + p) - 2\sqrt{\frac{(\mu + p)^3}{\phi}}$$

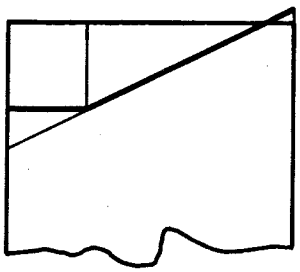

(c) Compression Yield Regime

$(\phi_{ec} < \phi_{et} \quad \phi_{ec} < \phi \le \phi_{ct})$

$$m = 3(1 - p) - 2\sqrt{\frac{(1-p)^3}{\phi}}$$

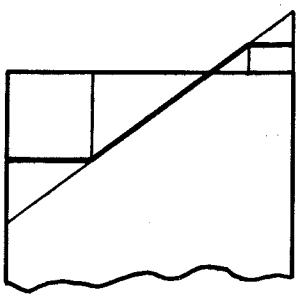

(d) Combined Yield Regime

$(\phi_{tc} < \phi \text{ or } \phi_{ct} < \phi)$

$$m = \frac{3(1-p)(\mu+p)}{1+\mu} - \frac{(1+\mu)^3}{16\phi^2}$$

Fig. 4 m-φ-p Equations in Regimes

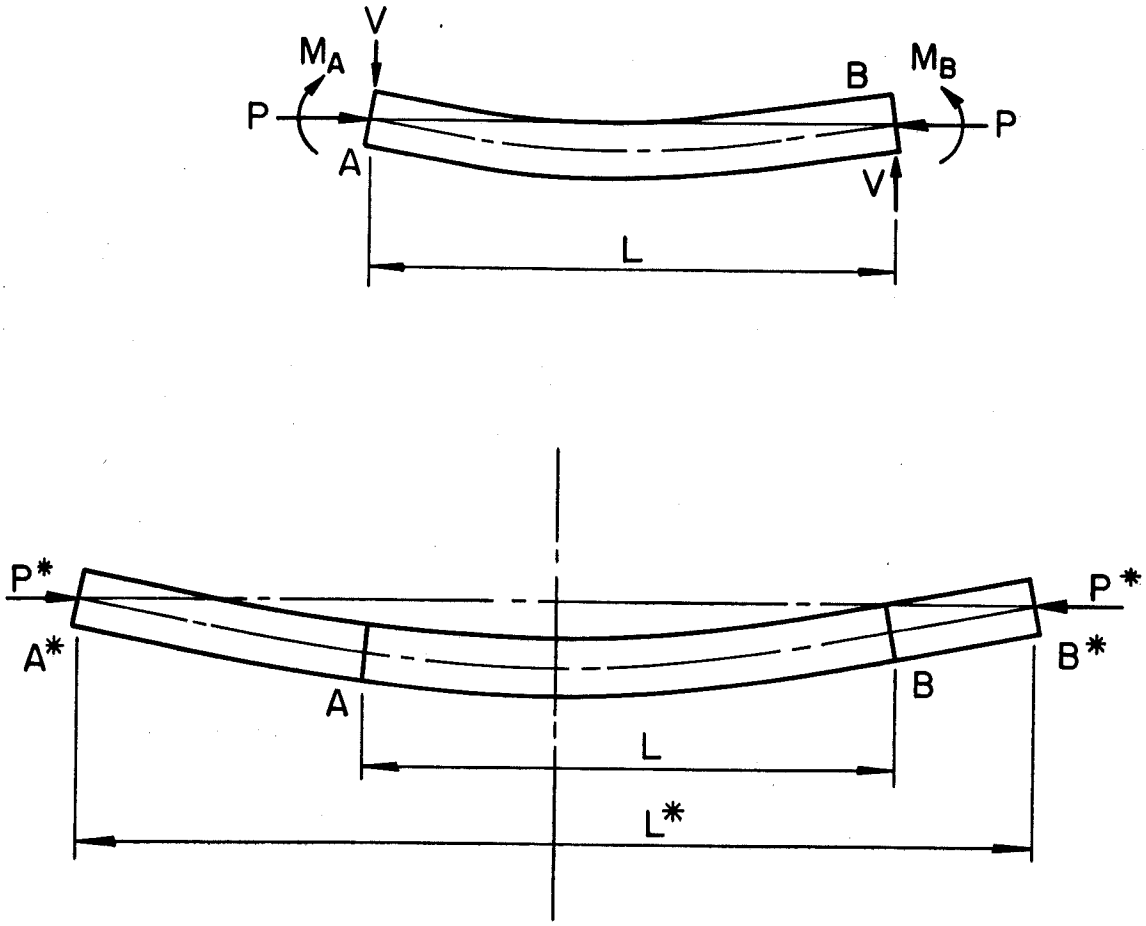

Fig. 5 Beam-Column and Its Equivalent Column

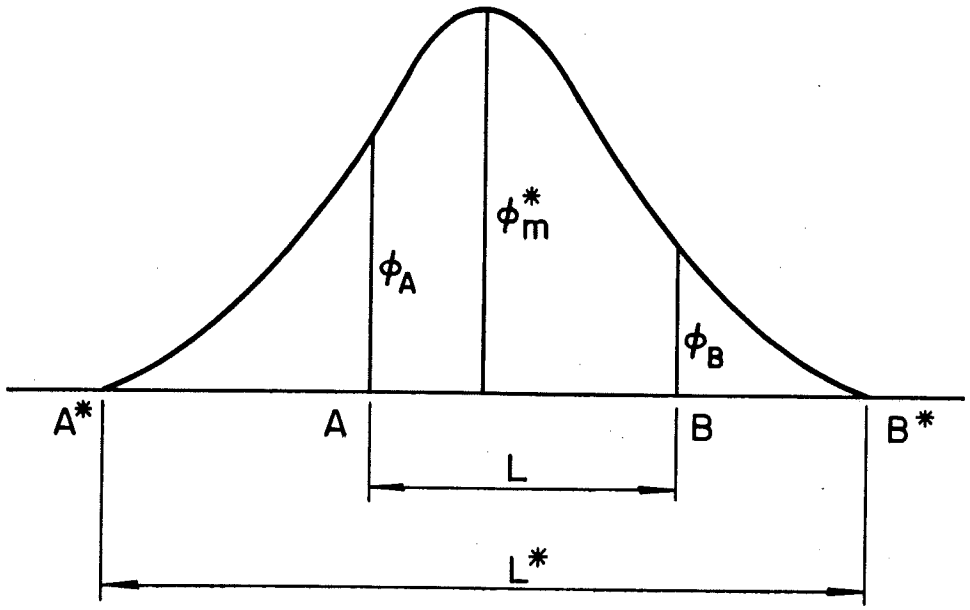

Fig. 6 Curvature of Beam-Column AB

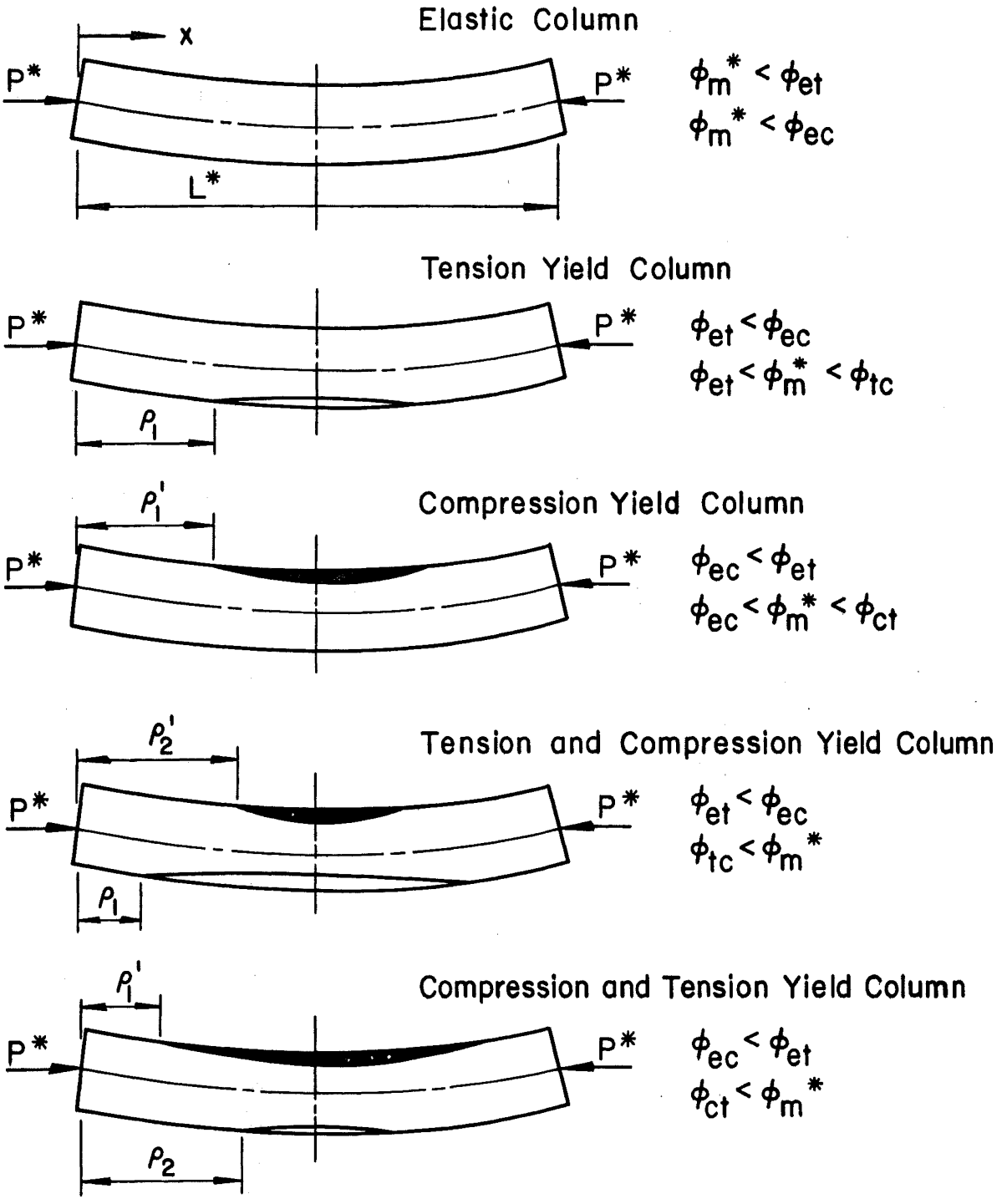

Fig. 7 Five Types of Equivalent Column

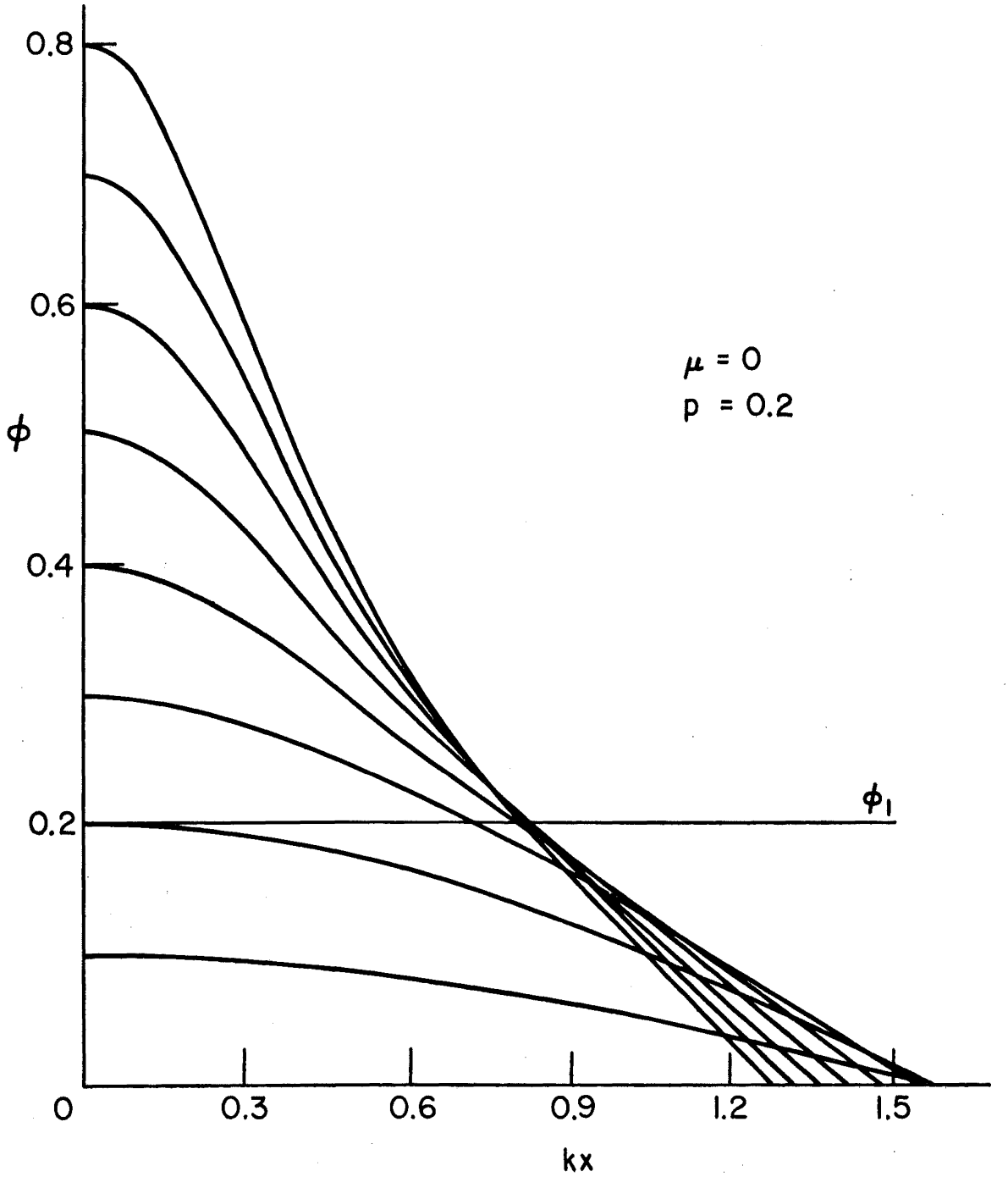

Fig. 8 Column Curvature Curves

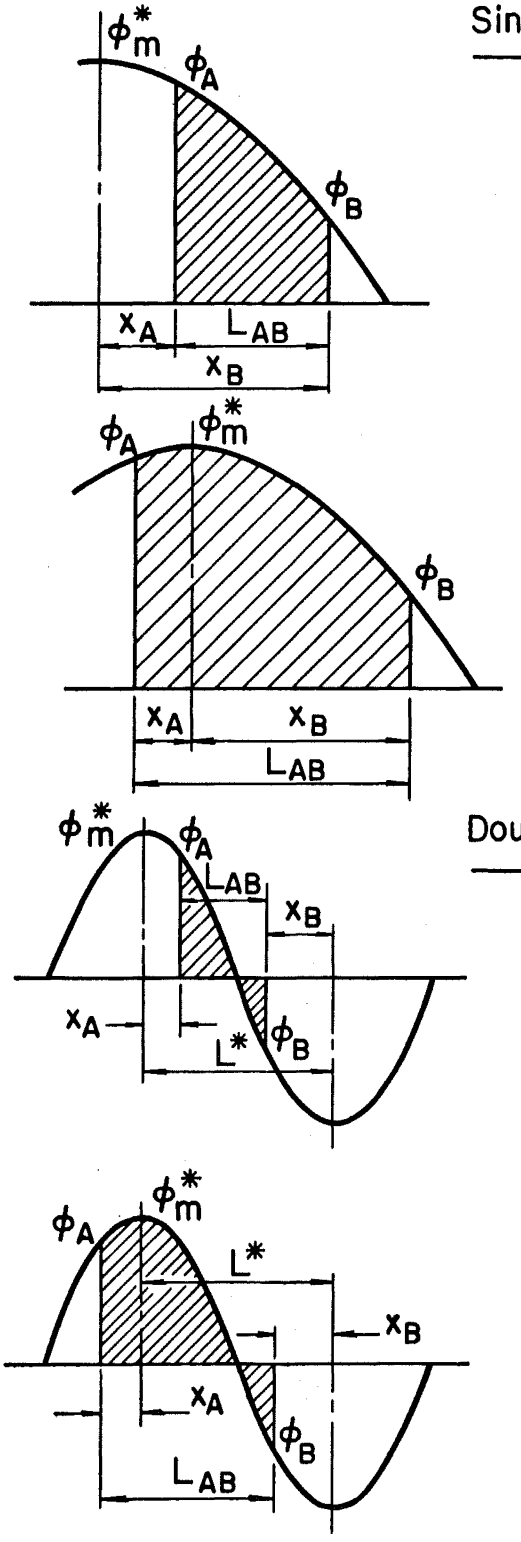

Single Curvature ($\phi_A \phi_B \geq 0$)

Type 1

$L_{AB} = x_B - x_A$

$\phi_m = \phi_A$, $x_m = 0$

Type 2

$L_{AB} = x_A + x_B$

$\phi_m = \phi_m^*$, $x_m = x_A$

Double Curvature ($\phi_A \phi_B < 0$)

Type 1

$L_{AB} = L^* - x_A - x_B$

$\phi_m = \phi_A$, $x_m = 0$

Type 2

$L_{AB} = L^* + x_A - x_B$

$\phi_m = \phi_m^*$, $x_m = x_A$

Fig. 9 Computation of Column Length L_{AB}

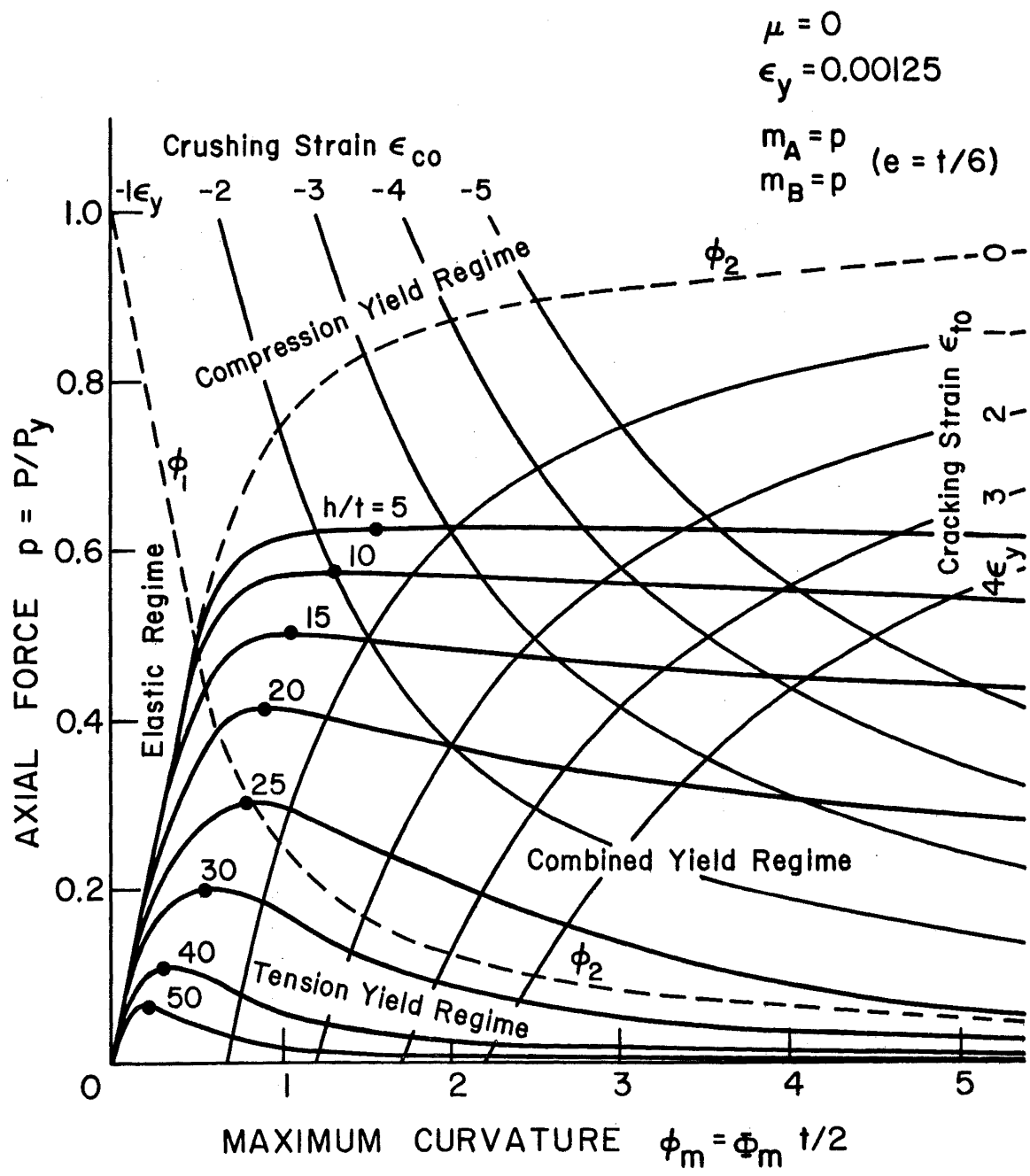

Fig. 10 Load-Curvature Curves of Masonry Wall

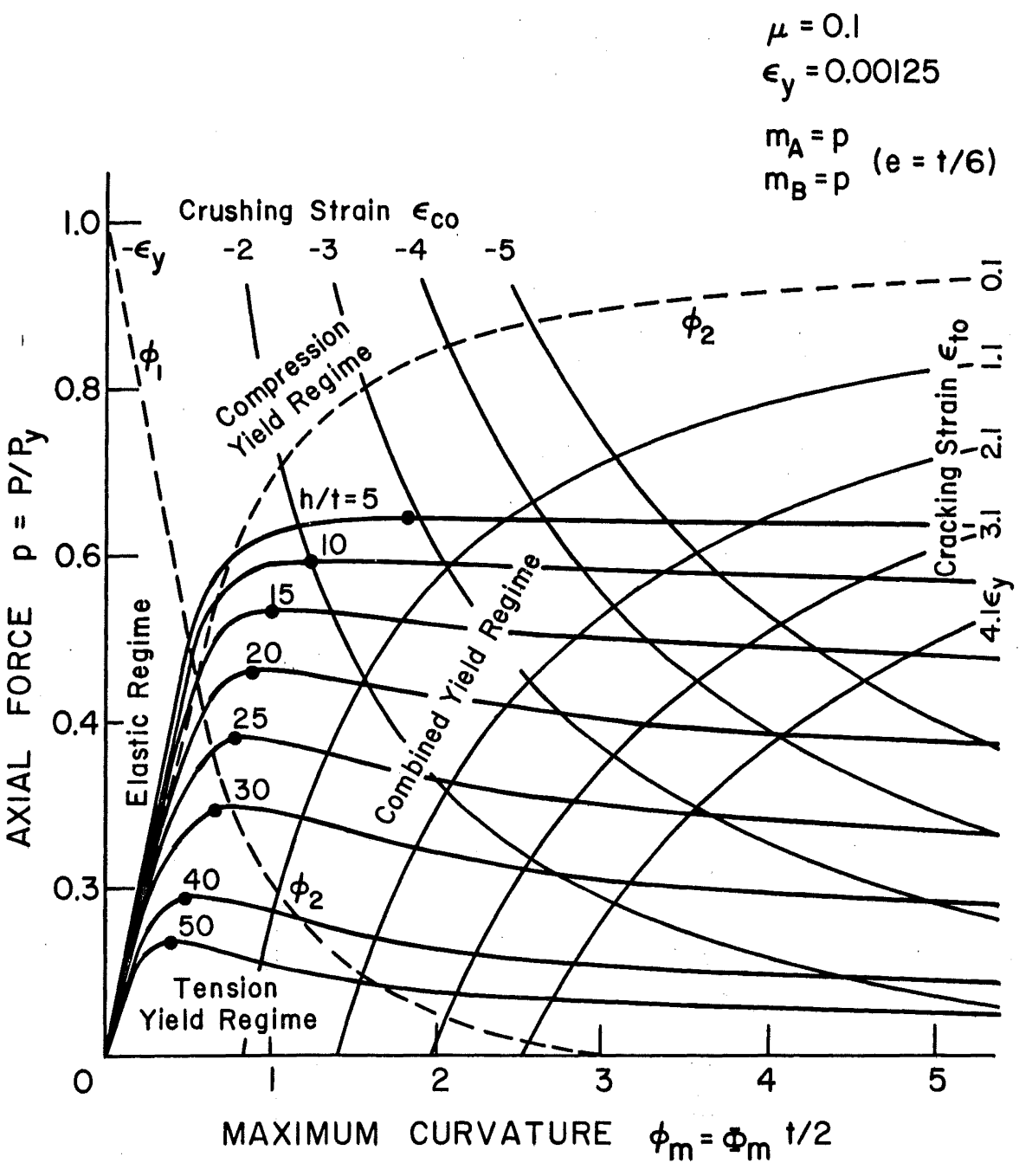

Fig. 11 Load Curvature Curves of Concrete Walls

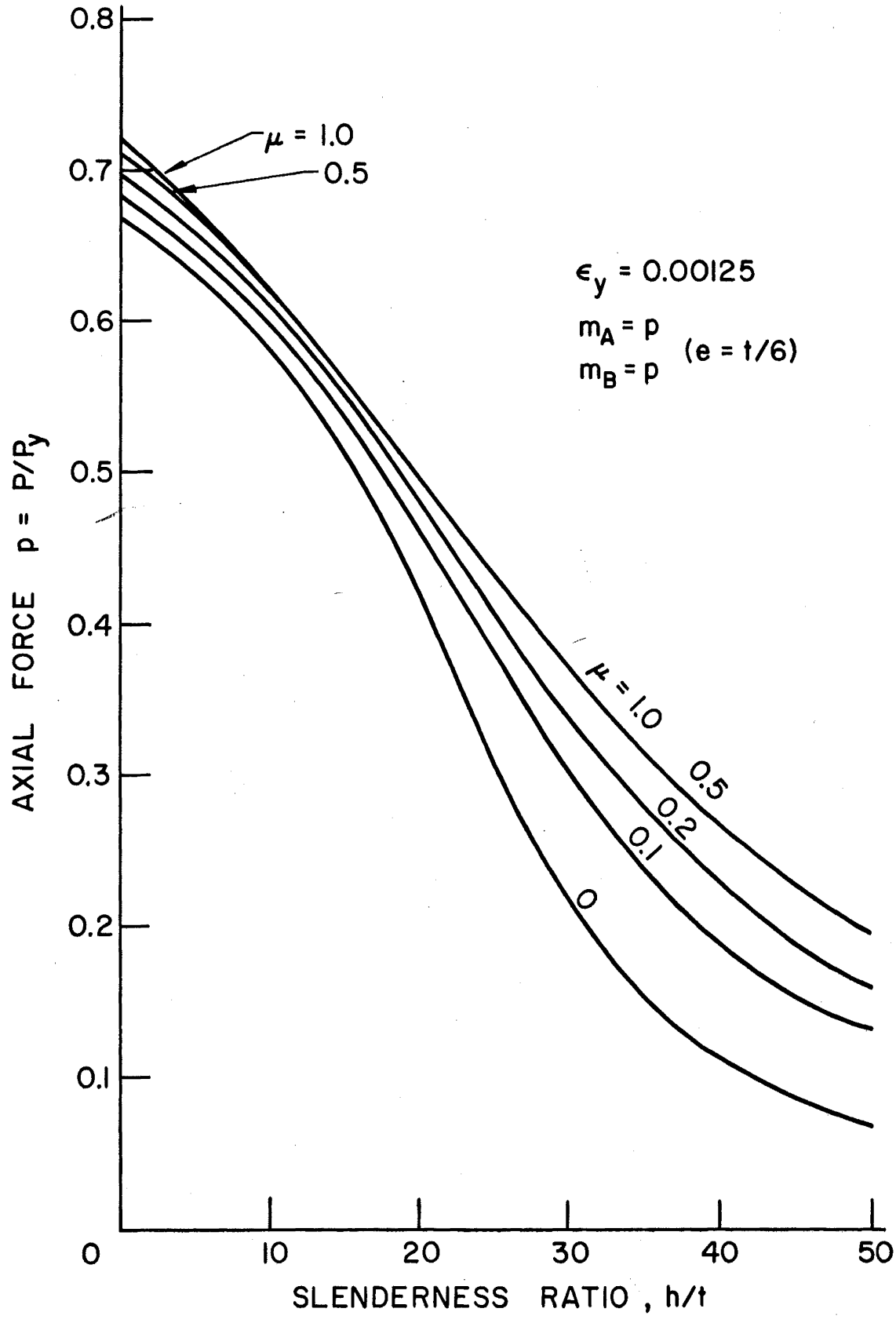

Fig. 12 Strength of Wall with Various Materials

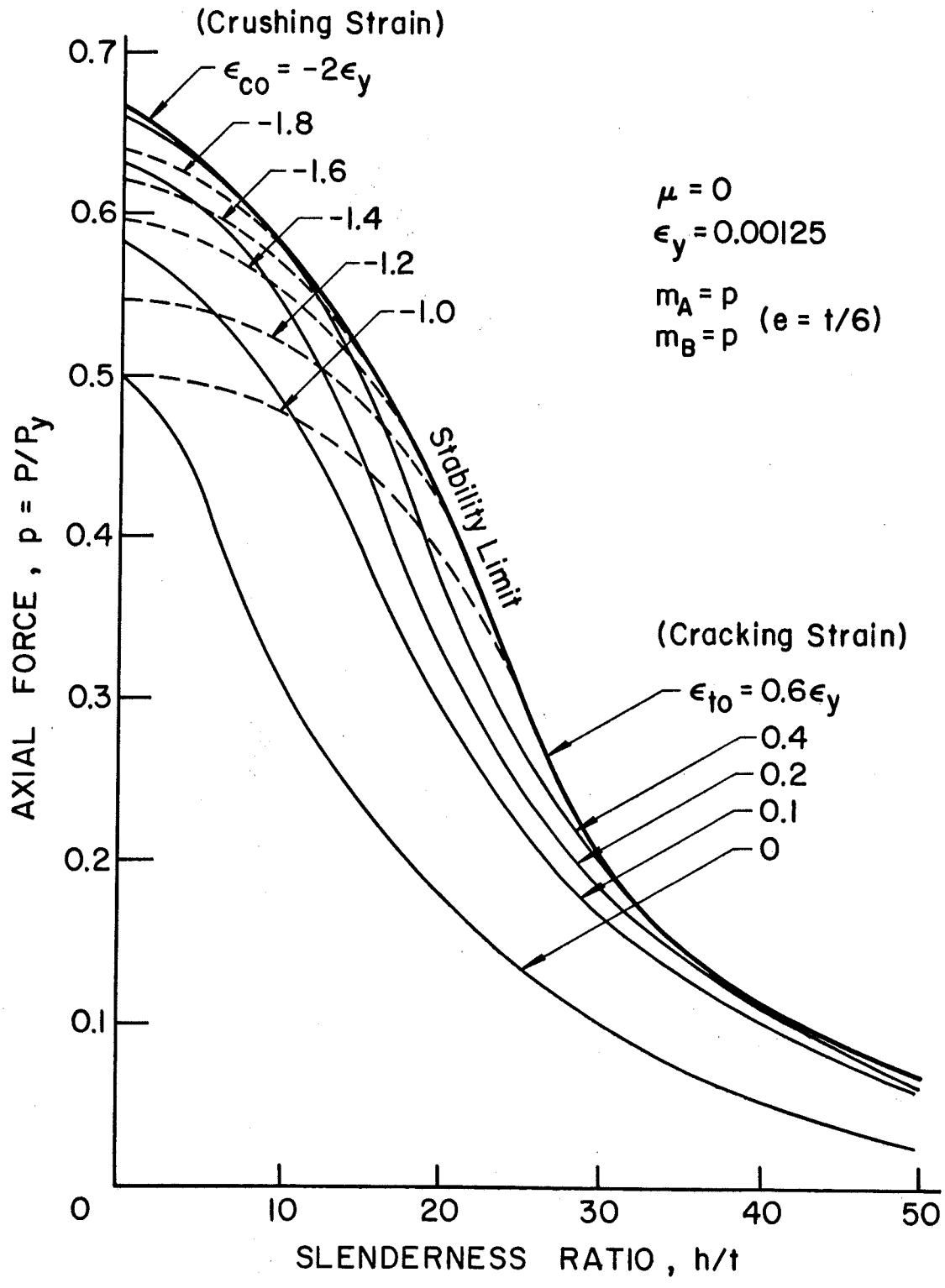

Fig. 13 Ultimate Strength due to Strain Limits

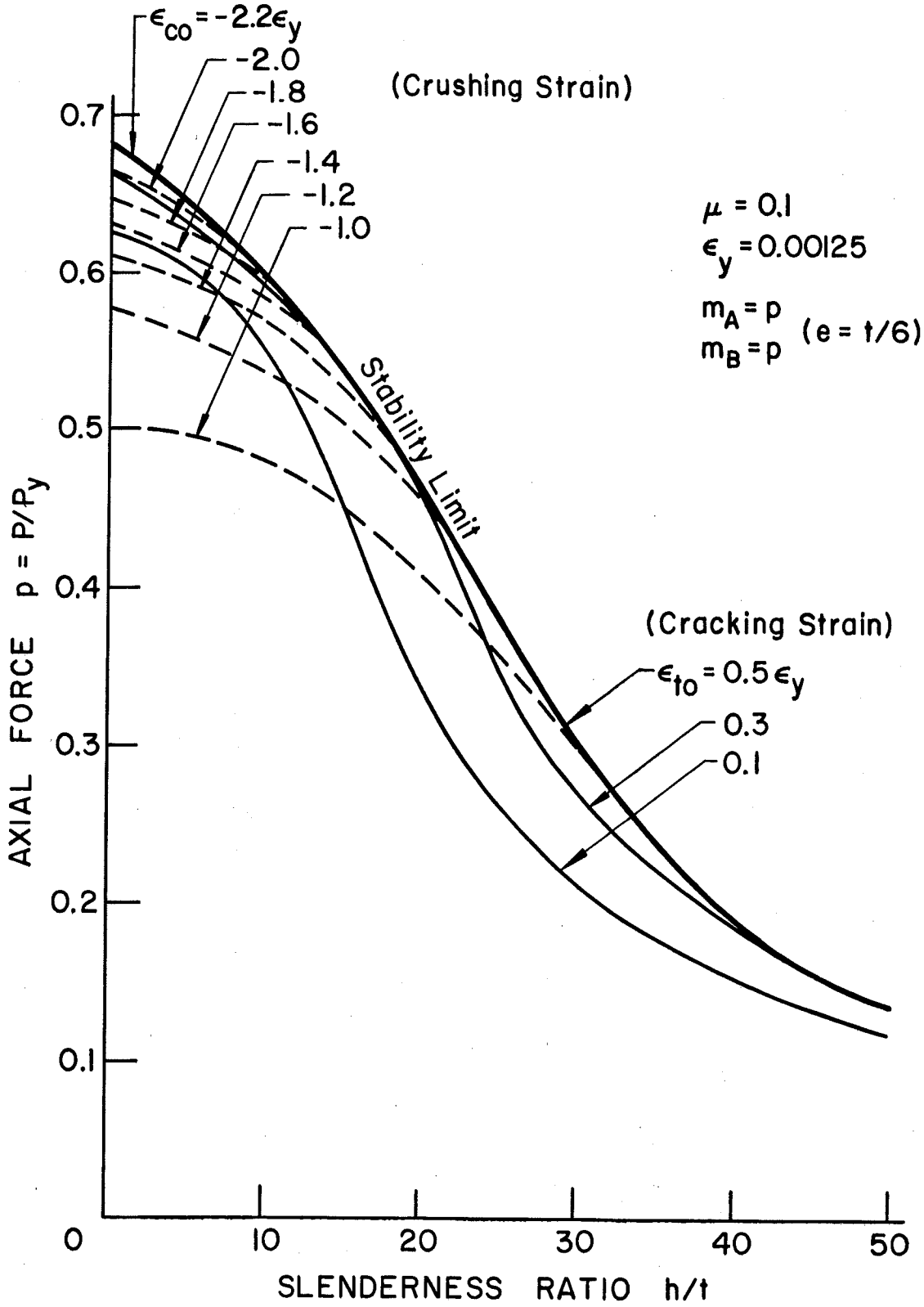

Fig. 14 Ultimate Strength due to Strain Limits

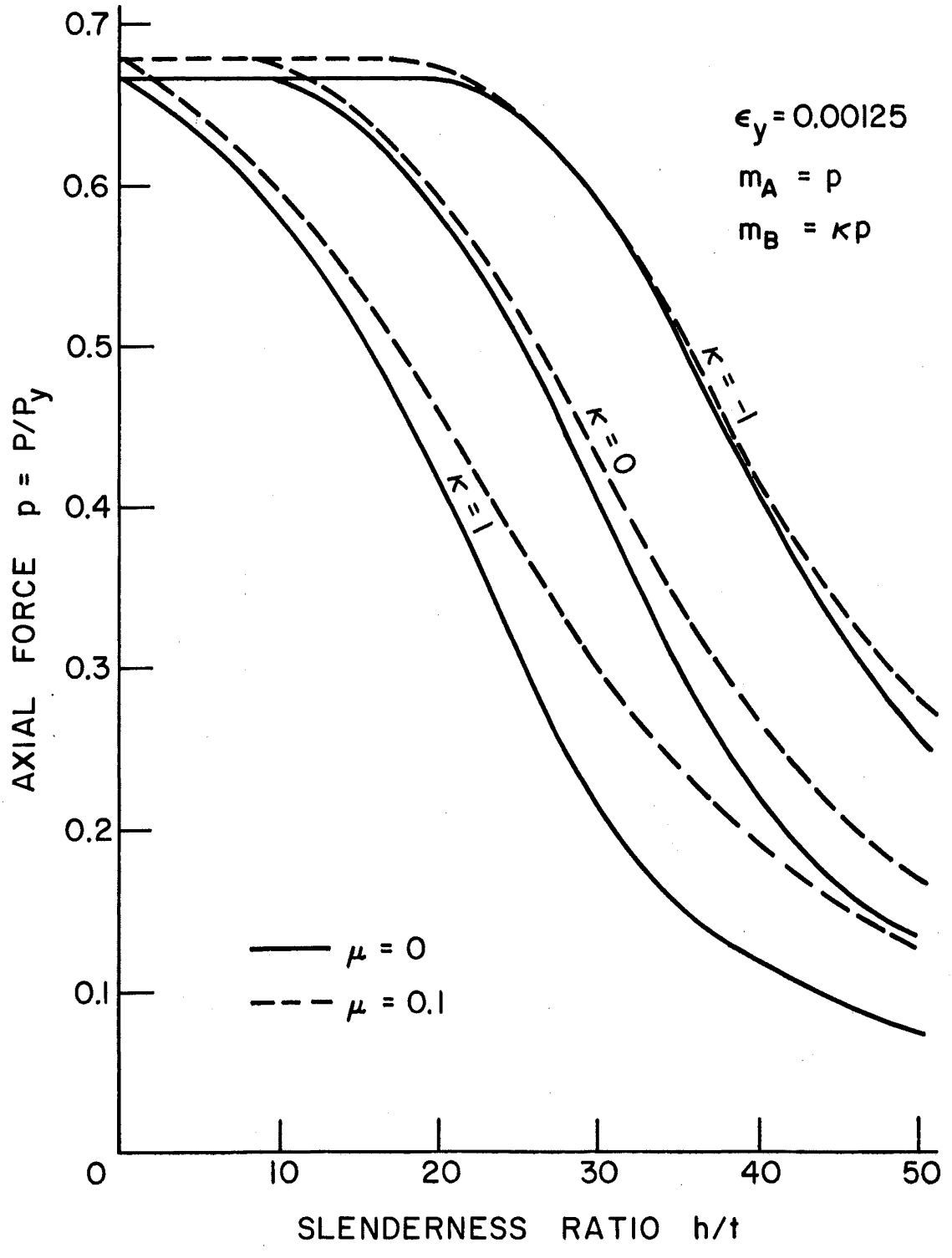

Fig. 15 Strength of Wall Against Various Types of Loading

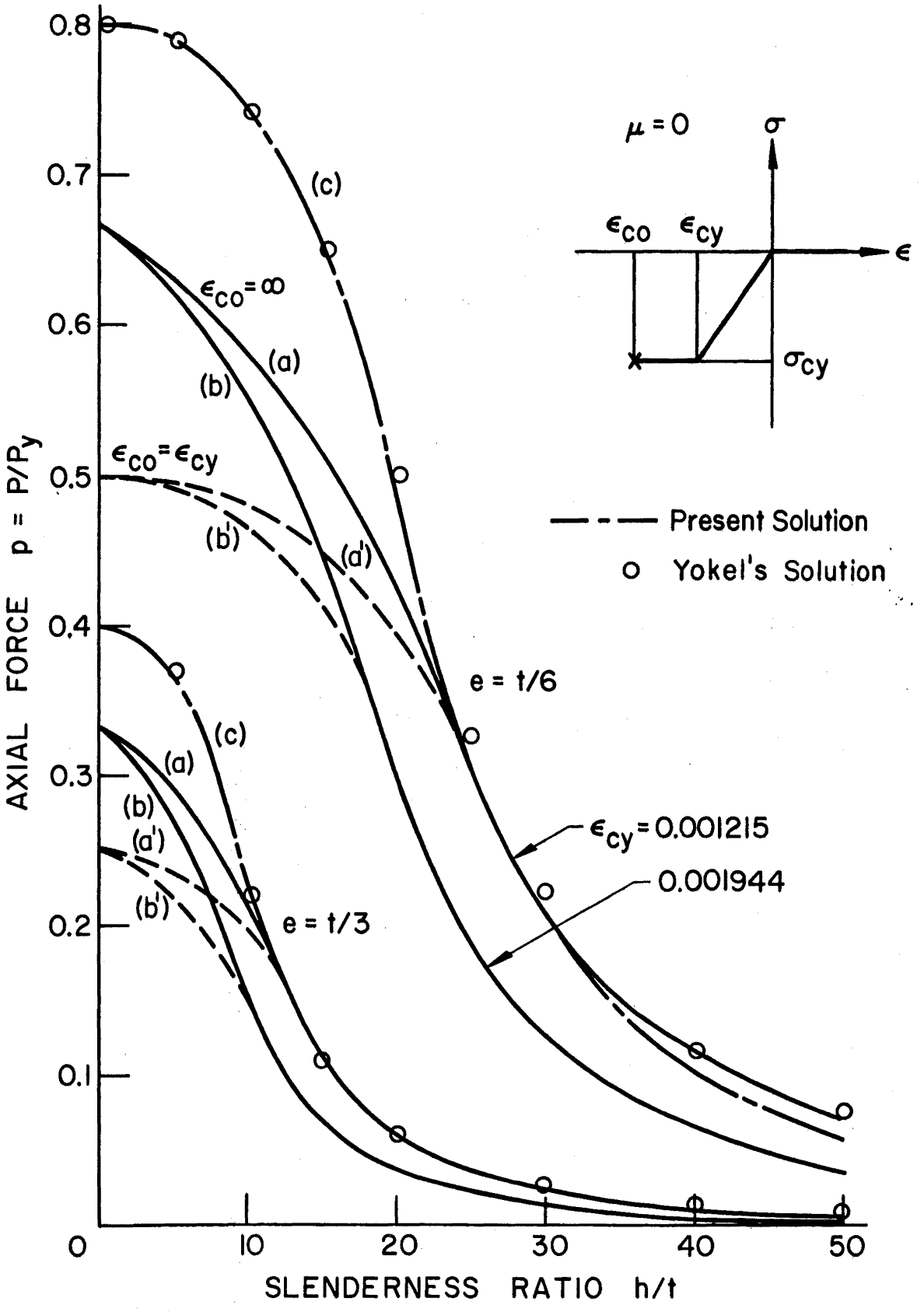

Fig. 16 Comparison with Reference 4